RSC Sustainability

ROYAL SOCIETY OF CHEMISTRY

PAPER

View Article Online
View Journal | View Issue

Cite this: *RSC Sustainability*, 2023, **1**, 2287

Towards sustainable synthesis: a life cycle assessment of polymer of intrinsic microporosity (PIM-1) by green mechanosynthesis†

Ching Yoong Loh, [a] Rui Huang,[b] Roy Bell[c] and Ming Xie *[a]

Received 22nd September 2023
Accepted 25th October 2023

DOI: 10.1039/d3su00340j

rsc.li/rscsus

Mechanochemistry represents an emerging technology that facilitates chemical reactions through the application of mechanical energy. This straightforward technique enhances reaction efficiency, expediting the process in an environmentally friendly, solvent-free manner. Polymers of intrinsic microporosity (PIMs) belongs to a class of polymers characterized by intrinsic microporosity, remarkable processability, and high adsorption capacity, rendering them well-suited for gas-related applications. However, conventional wet chemical synthesis methods of PIM-1 often necessitate substantial solvent usage, leading to significant and enduring environmental impacts. In this study, we present an alternative approach, harnessing green mechanochemical reactions to produce PIM-1. Furthermore, we conducted a comprehensive Life Cycle Assessment (LCA) to compare and simulate the environmental impacts of both wet chemical and mechanosynthesis methods. Our findings indicate the successful qualitative synthesis of PIM-1 through mechanochemistry, resulting in a notable reduction of environmental impacts, approximately 1.5 times less compared to the conventional wet chemical synthesis route. This advancement holds great promise for advancing sustainable and eco-friendly polymer synthesis methods.

Sustainability spotlight

Polymer of intrinsic microporosity (PIM) has major implications with gas applications and high potential in the fabrication of liquid separation membranes as a material. However, in principle, the synthesis of the highly adsorptive material rely on wet chemical methods, which poses a hazard to the environment due to the involvement of toxic chemicals with exceeding amount. As a notable alternative, mechanosynthesis has emerged as a green technology that minimizes or eliminates the need for solvents, thereby substantially reducing the adverse environmental impacts associated with chemical reactions. In our research, we have successfully synthesis PIM-1 *via* mechanochemistry reaction, involving minimal solvents in the process. Furthermore, we conducted a comprehensive environmental assessment employing the Life Cycle Assessment (LCA) method, which showed that the former generates more negative impact to the environment. This study aligns seamlessly with the United Nations Sustainable Development Goals (SDGs), particularly emphasizing for responsible consumption and production (SDG 12), life below water (SDG 14) and life on land (SDG 15).

1 Introduction

Polymers of intrinsic microporosity (PIMs) is a distinctive class of porous materials that exhibit great potential as adsorbents in physical adsorption processes.[1] Unlike conventional polymers, which typically possess tightly packed structures with limited void space due to strong intermolecular forces, PIMs demonstrate a remarkable deviation by offering significant internal voids. These voids form a continuous network of interconnected intermolecular spaces, giving rise to the term 'intrinsic microporosity' and endowing the material with unique microporous characteristics.[2,3] This intrinsic microporosity grants PIMs significant microporous characteristics, allowing them to act as molecular sieves. Among the various PIMs, PIM-1 stands out due to its excellent solubility in solvents like chloroform and tetrahydrofuran (THF), enabling its transformation into different forms, from granules to films.[4] Additionally, PIM-1 demonstrates high surface areas and remarkable adsorption capacities.[5] Consequently, PIM-1 has found wide-ranging applications in fields such as hydrogen storage,[6] gas separation,[7] and energy storage,[8] owing to its unique properties and versatility.

PIM-1 can be synthesized through two primary methods: the low-temperature method,[1] and the high-temperature method.[9] More recently, Zhang *et al.*[10] proposed an alternative synthesis approach utilizing a mechanochemical reaction that remarkably reduces the synthesis time to just 15 minutes. This method involves initially combining the reactants, namely 5,5′,6,6′-tetrahydroxy-3,3,3′,3′-tetramethyl-1,1′-spirobisindane (TTSBI) and

[a]*Department of Chemical Engineering, University of Bath, Bath, BA2 7AY, UK. E-mail: m.xie2@bath.ac.uk*

[b]*Guangdong Water Co., Ltd, Shenzhen, China, 518001*

[c]*PA Consulting, 50 Farringdon Rd, London EC1M 3HE, UK*

† Electronic supplementary information (ESI) available. See DOI: https://doi.org/10.1039/d3su00340j

tetrafluoroterephthalonitrile (TFTPN), along with the addition of K_2CO_3 as a catalyst. The reaction mixture, along with suitable balling media, is then subjected to grinding in a ball milling machine. Notably, the conventional low-temperature and high-temperature methods typically require 24–72 h for PIM-1 synthesis, whereas the mechanochemical approach achieves a significantly shorter reaction time, yielding PIM-1 with a remarkable 98% efficiency.[10]

On the other hand, mechanochemistry, as an emerging technology, has gained prominence in the field of green chemistry over the past decade.[11] Defined by IUPAC as 'chemical reactions induced by mechanical energy,[12] mechanochemistry often takes place without the need for solvents, making it a sustainable and environmentally friendly approach. Moreover, it has been utilized extensively, especially in the environmental sector, for instance, refining fly ash,[13–15] reducing carbon dioxide,[16–18] and dye adsorption.[19–21] Therefore, employing mechanochemistry in the synthesis of PIM-1 not only offers significant time savings but also aligns with sustainable and green principles.

Mechanosynthesis has emerged as a promising green technology. However, the carbon footprint, particularly the environmental implications of this method has not been quantitatively analyzed, necessitating a thorough evaluation of its environmental impacts for informed decision-making regarding PIM-1 synthesis or, more broadly, other reactions and processes. In general, there are several metrics in green chemistry that could be utilized to quantitatively evaluate the environmental impacts, including atom economy, environmental factor, process mass intensity.[22] The evaluation of these metrics could potentially promote the development of green technologies in laboratories and industries. Moreover, there are also generic assessments such as Life Cycle Assessment (LCA)[23,24] or DOZN 2.0 (ref. 25) that are used extensively for the evaluations of environmental impacts of chemical processes. LCA is a widely employed quantitative tool, both in commercial and academic settings, to assess the environmental impacts of a given subject. It encompasses the evaluation of impacts occurring throughout the entire product life cycle, spanning from raw material extraction to product disposal.[26] LCA serves to prevent the potential over-interpretation of environmental burdens during the development stages of a synthesis method.[27] By providing a comprehensive and quantitative approach, LCA facilitates comparative studies and offers valuable insights into the environmental implications of various methods, fostering a more comprehensive understanding of their environmental impacts. In the context of PIM-1, Goh *et al.* had recently evaluated the environmental impacts of PIM-1 production as membrane materials using LCA.[28] The group assessed the conventional low-temperature and high-temperature method of PIM-1 synthesis, emphasizing on solvent recovery and choosing alternative monomer.

In this study, we explored mechanosynthesis by synthesizing PIM-1 *via* mechanochemical reaction and further evaluate the environmental impacts of mechanosynthesis *via* LCA. This will provide a comprehensive understanding of the environmental performance of mechanochemistry and its potential as a sustainable synthesis approach for PIM-1 polymer and beyond. The findings of this study will contribute to the broader discussions on green synthesis methods and support the development of environmentally friendly strategies in materials science and chemistry.

2 Materials and methodology

2.1 Chemicals and materials

TTSBI (97%), TFTPN (98%), and potassium carbonate (anhydrous, 98%), were purchased from Alfa Aesar. Ethanol (analytical grade) was purchased from Fischer Scientific, and methanol (analytical grade) was purchased from VWR. De-ionized water was used for any aqueous usage and solution preparation.

2.2 Green mechanosynthesis of PIM-1

PIM-1 was synthesized using TTSBI, TFTPN, and K_2CO_3 as reactants *via* mechanochemistry.[10] The molar ratio of these reactants was set to 0.5 mmol : 0.5 mmol : 1.5 mmol, which corresponded to a near-complete synthesis reaction. All reactants were added into a stainless-steel reactor, with stainless-steel ball bearings. The stainless-steel reactor was placed into a Retsch PM 200 planetary ball mill (750 W, 500 rpm) for 20, 40 and 60 min to study the reaction kinetics of the synthesis of PIM-1. The reactant-to-ball ratio was controlled (1 : 64 and 1 : 128). The mixture resulting from the grinding procedure was collected and washed repeatedly using ethanol, methanol, and de-ionized water after centrifuge purification. After washing, the compound was dried by placing it on a watch glass in the oven overnight at a temperature of 55 °C. The resulting solids were sampled for characterization and were denoted as PIM-1.

2.3 Characterization of PIM-1

Proton nuclear magnetic resonance (^{1}H NMR) analyses with samples dissolved in deuterated chloroform were performed (400 MHz Bruker NMR Spectrometer, Massachusetts, USA). Fourier-transform infrared (FT-IR) spectroscopy (PerkinElmer FT-IR Spectrometer Frontier, Massachusetts, USA) was performed to record the infrared spectra of the surface to determine the succession of the material deposits. The spectral resolution was 4 cm^{-1}, and 16 scans were recorded for spectrum ranging from 4000–400 cm^{-1} for each sample after background analysis. Gel-Permeation Chromatography (GPC) was performed to determine the average molecular weight of the synthesized polymer. The PIM-1 samples were dissolved in THF, with a calibration standard of polystyrene. Scanning electron microscopy (SEM) was performed to study the overall morphology of PIM-1. The samples were degassed in a pressurized chamber overnight to remove unwanted particles for better imaging. The samples were coated with a layer of gold before carrying out SEM (Hitachi SU3900, Kyoto, Japan) to minimize a charge build-up in the sample. Brunauer–Emmett–Teller (BET) surface area analysis (Autosorb-iQ-C, Graz, Austria) was carried out to measure the specific surface area of the mechanosynthesis PIM-1. The samples were weighed and later

degassed at 120 °C for 16 h before starting the analysis of adsorption and desorption isotherm with N_2.

2.4 LCA study of mechanosynthesis and wet chemical method

Life cycle assessment (LCA) was conducted between mechanosynthesis and wet chemical method for PIM-1 synthesis. OpenLCA (version 1.10.3) was utilized as a calculation and modelling software tool to further evaluate the report. The database, Eco-Invent 3.7 was used to provide necessary information on the inventory inputs and outputs of the assessment. In the final part of the modelling process, ReCiPe 2016 'H' midpoint analysis was employed for the impact assessment section.

In the assessment, the "cradle-to-gate" analysis technique was utilized to examine the chemical process of mechanochemical reaction and wet chemical reaction in the synthesis of PIM-1. Table 1 illustrated the experimental procedures of both mechanosynthesis and wet chemical method to produce PIM-1. The functional unit of this LCA report was assumed to be 1.0 g. To further elaborate, a competent contrast between the two methods was made by considering the production yield. Fig. 1 showed the system boundary of both mechanosynthesis and wet chemical method in the LCA model simulation.

2.4.1 Life cycle inventory (LCI) analysis. The LCA inventories were modelled and simulated based on the inputs in Table S1.† Energy consumption was calculated using equipment energy ratings, and washing chemicals were assumed at a 10 mg product/1 ml chemical scale. Centrifuge time for washing was assumed as 15 min per wash, per chemical, with three repeating cycles. The functional unit for assessment was set as 1 g of PIM-1 for both synthesis methods. These approaches enabled a direct and fair comparison of the environmental impacts. LCA provides a systematic and quantifiable approach to assess environmental implications, considering factors such as energy consumption and chemical usage. Reliable input data and reasonable assumptions are crucial for accurate LCA results. Overall, LCA inventories facilitated evaluation, decision-making, and improvement of sustainable synthesis processes.

2.4.2 Life cycle impact analysis (LCIA). ReCiPe was selected as the LCIA method for this comparative LCA, focusing on midpoint assessment categories to capture the most significant environmental impacts. ReCiPe offers 18 midpoint indicators and 3 endpoint indicators, derived from its precursors CML 2000 and Eco-indicator 99. The assessment utilized ReCiPe (2016) midpoint (H) with a normalization package of World (2010) H. "H" represents the hierarchist cultural perspective, which is widely recognized as the default and consensus model among the three cultural perspectives.[30]

3 Results and discussion

3.1 Key physicochemical properties of mechanosynthesized PIM-1

The successful mechanosynthesis of PIM-1 was visually confirmed through significant color transformation of the reactants, as depicted in Fig. 1a and b. Initially, the reactants exhibited a white powder appearance, which underwent a noticeable change to a yellow powder state, indicating the formation of PIM-1.

The NMR analysis of the PIM-1 samples exhibited sharp peaks, demonstrating the solubility of PIM-1 in deuterated chloroform ($CDCl_3$) as the solvent (Fig. 1c). The functional groups of the PIM-1 structure were assigned with the corresponding peaks in the NMR spectra (Fig. 2b and c). Notably, distinct peaks at 6.4 and 6.8 ppm were observed, which was attributed to the aromatic group presented in PIM-1.[1,10]

The NMR results revealed that the formation of PIM-1 was already evident after 20 minutes of the synthesis process, as evidenced by the identical NMR spectra obtained at different time intervals (40 min and 60 min) (Fig. S1†). Moreover, a comparison of the NMR spectra between samples with reactant-ball mass ratios of 1 : 64 and 1 : 128 indicated no significant differences, suggesting that both samples represent the same compound (Fig. S2†).

The FT-IR spectra displayed in Fig. 1d showed the functional group analysis of PIM-1 synthesized using a 1 : 64 reactant-ball ratio at 60 min. Notably, a peak observed at 2200 cm^{-1} confirmed the presence of the nitrile group (C–N) characteristic of PIM-1. Additionally, the absence of a peak in the range of 3000–3700 cm^{-1}, where the alcohol O–H group from the TTSBI monomer would typically peak,[1] further supported the identification of the product as PIM-1. The identical FT-IR spectra obtained for the three samples at different time intervals

Table 1 Mechanosynthesis and wet chemical method synthesis of PIM-1

	Mechanosynthesis	Wet chemical method
Material inputs	TTSBI ($C_{21}H_{24}O_4$), TFTPN (C_6F_4-1,4-$(CN)_2$), potassium carbonate (K_2CO_3), ethanol (C_2H_5OH), methanol (CH_3OH), de-ionized water (H_2O)	TTSBI ($C_{21}H_{24}O_4$), TFTPN (C_6F_4-1,4-$(CN)_2$), potassium carbonate (K_2CO_3), dimethyl sulfoxide ($(CH_3)_2SO$), toluene ($C_6H_5CH_3$), ethanol (C_2H_5OH), de-ionized water (H_2O)
Energy inputs	Ball milling for 60 min, washing with ethanol, methanol and de-ionized water using a centrifuge, drying with oven for 24 h	Stirring for 3 min pre-reaction, heating and stirring for 8 h, washing with ethanol and de-ionized water using a centrifuge, drying using an oven for 24 h
Functional units	1 g of PIM-1	1 g of PIM-1
Yield	98%	93%
Reference	Zhang *et al.*,[10] experimental data from this study	Ponomarev *et al.*[29]

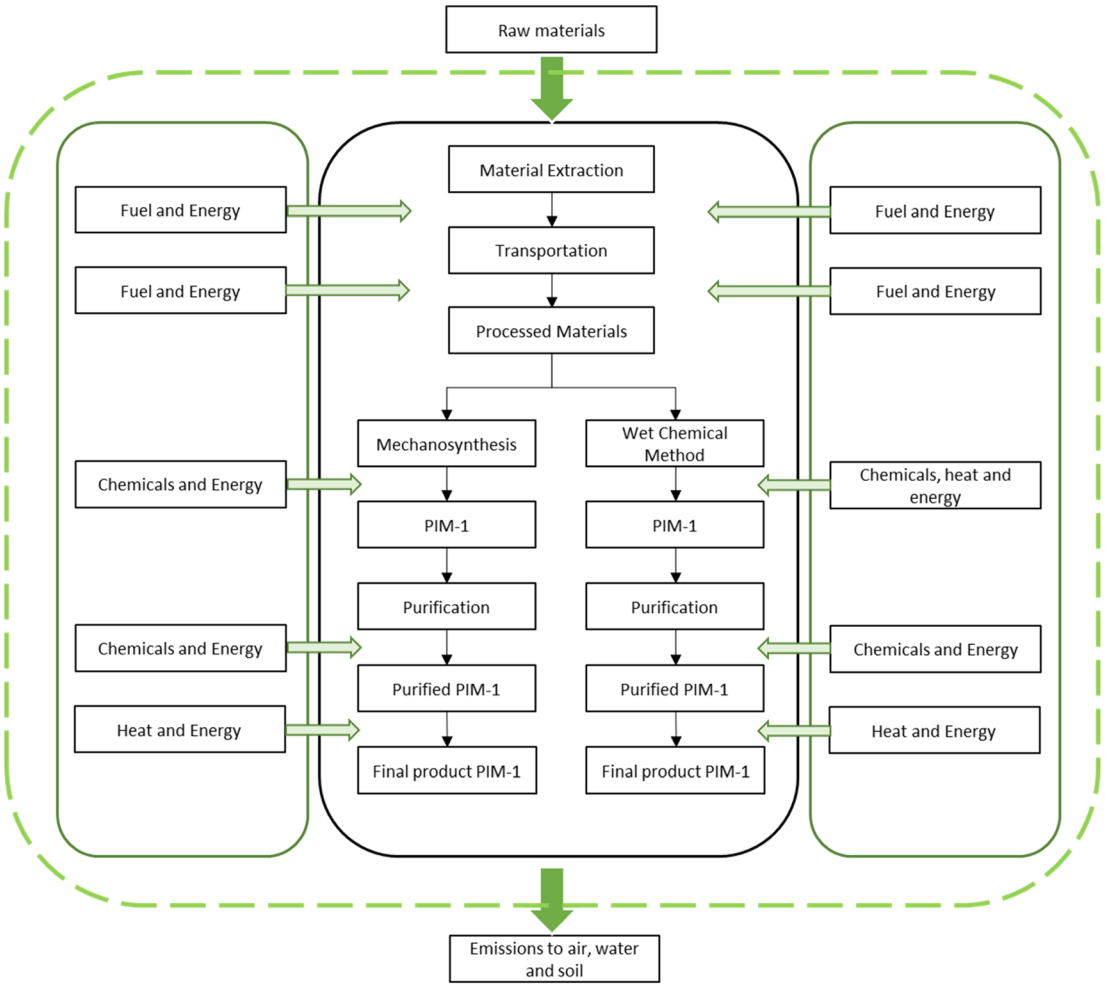

Fig. 1 The system boundary of mechanosynthesis and wet chemical reaction of PIM-1 synthesis.

(Fig. S3†) confirmed that all samples were the same product. Furthermore, the intensity of the peaks increased proportionally with the reaction time, suggesting that the reaction progressed as the duration extended.

The PIM-1 morphology and polymer structure were imaged in Fig. 1e, illustrating the microporous characteristics of the mechanosynthesized polymer. The hierarchical pores from PIM-1 shown in the SEM images (indicated by the red circle) are the intrinsic pores that confirmed the success of the synthesized polymer.[31,32] Kinetics of the synthesis reaction is shown in Fig. S4.† At 20 min, the morphology of PIM-1 could still be seen as packed and there were no spaces between each PIM-1 particle (Fig. S4a†). Hence, the polymerization of PIM-1 was not complete because of the lack of free volume of the polymer that should be resulting in micropores. However, the voids became more obvious at the 40 min (Fig. S4b†) and finally, the pore structures were visible after 60 min (Fig. 1e). Regarding the case of the 1 : 128 reactant-ball ratio, as shown in Fig. S4d,† the voids in each 'granule' of PIM-1 were smaller and appeared more frequently. This phenomenon proves that the greater the ball mass, the greater its efficiency and efficacy on the synthesis, and in this case, the overall surface area of the sample increases. The structure of these PIM-1 samples has slightly bigger void spaces and tighter packing formation, resulting in fewer surface areas. This could be attributed to the nature of the synthesis method, where there were enhanced polymer cohesion and packing during the progress of the reaction involving grinding of the solid-state.[10,33]

Table 2 presents the molecular weight of various PIM-1 samples. It is observed that a shorter polymerization time of 20 minutes results in a lower molecular weight of PIM-1, a consequence of the reduced time available for the polymerization of monomers. In contrast, after a duration of 60 minutes, the polymerization of PIM-1 appears more comprehensive. Specifically, at reactant-to-ball ratios of 1 : 64 and 1 : 128, the average molecular weight (M_w) reached 41 000 g mol^{-1} and 60 991 g mol^{-1}, respectively. While applications, particularly in membrane fabrication, often favor PIM-1 with a high molecular weight (>100 kg mol^{-1}),[34,35] it's noteworthy that Bhavsar *et al.* demonstrated the feasibility of CO_2 gas separation membranes using PIM with an M_w of approximately 50 kg mol^{-1} by grafting polyethylene oxides onto PIM-1.[35] Similarly, research by Kim

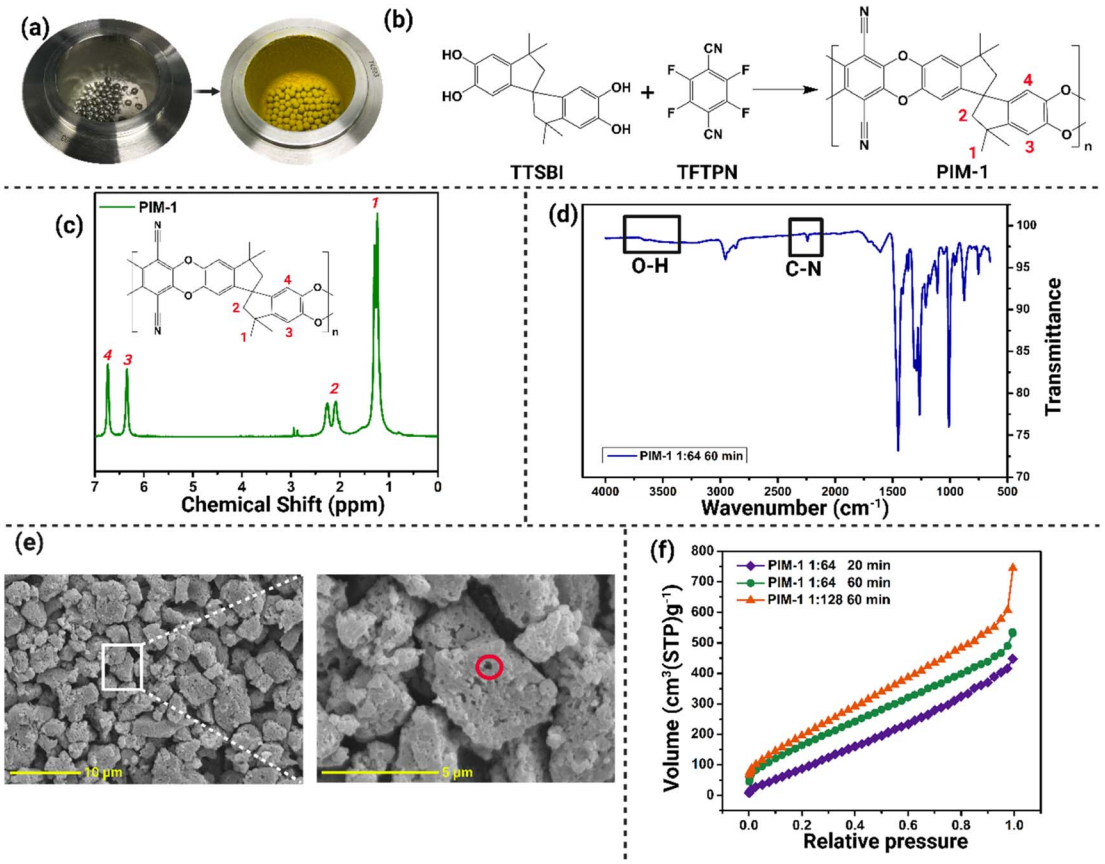

Fig. 2 (a) Photographic samples of PIM-1 before and after the reaction. (b) Schematic diagram of the molecular structure of PIM-1 with the assigned functional groups of the NMR spectra. (c) NMR spectra, (d) FT-IR spectra, (e) SEM image and (f) adsorption isotherm for PIM-1 at different conditions.

and colleagues showcased the use of PIM-1, with an M_w of 50 100 g mol^{-1}, in the fabrication of carbonaceous membranes suited for saline water treatment.[36]

3.2 Adsorption/desorption isotherms

Based on the IUPAC classification of adsorption isotherms, the adsorption/desorption isotherms of the mechanosynthesized PIM-1 (Fig. 1f and S5†) can be characterized as a composite of type I and type IV isotherms. This suggests a porosity that bridges between the microporous and mesoporous scales. In comparison to conventionally synthesized PIM-1, the ambiguous nature of the adsorption curve—oscillating between type I and type IV characteristics—might be attributed to suboptimal polymerization during the mechanosynthesis process. This inefficiency could result in increased free spaces among the monomers, thereby amplifying the porosity scale. The observations aligns with results from the SEM analysis, which further indicate that the PIM-1 samples manifest porosity at both macro and micro scales. Furthermore, the hysteresis of PIM-1 after 60 min exhibited a reduced magnitude compared to the PIM-1 at 20 min, as demonstrated in Fig. S5a and b.† As the level of hysteresis is subjected to the mesoporosity, this can be attributed to the reduction in mesoporosity of PIM-1 over the course of the reaction, which correlates with the kinetic profile of PIM-1 polymerization. Notably, under the condition of a 1 : 128 reactants-to-balls ratio (Fig. S5c†), the hysteresis approached closure. This suggests that increased mechanical force contributes to the enthalpy necessary for polymerization, thereby leading to a heightened microporosity. On the other hand, there is an unlinked hysteresis phenomenon occurring at lower relative pressure. This is caused by the elastic changes of the polymer segment positions and acting solvation pressures, which commonly occur in most microporous polymers.[37]

Table 2 Molecular weight of PIM-1

Reaction conditions	Number average molecular weight, M_n (g mol^{-1})	Average molecular weight, M_w (g mol^{-1})
PIM-1, 1 : 64, 20 min	2274	4806
PIM-1, 1 : 64, 60 min	21 939	41 028
PIM-1, 1 : 128, 60 min	14 644	60 991

Table 3 BET surface area of PIM-1

Reaction conditions	BET surface area (m^2 g^{-1})
PIM-1, 1 : 64, 20 min	545.1
PIM-1, 1 : 64, 60 min	710.1
PIM-1, 1 : 128, 60 min	855.5

Table 3 presents the BET surface area results of PIM-1 synthesized under different conditions. The analysis confirms that the resulting PIM-1 samples are microporous, falling within the typical range of 300–2000 m^2 g^{-1} for microporous materials.[38] In general, PIM materials exhibit surface areas ranging from 500–1000 m^2 g^{-1}.[1] The results support the hypothesis that surface area increases with reaction time in mechanosynthesis, where it can be attributed to the continuous molecular collisions between reactants and balls throughout the reaction, resulting in a higher adsorption surface area. Similarly, the BET surface area of the samples also correlates with the reactants to ball mass ratio, indicating that higher ball masses lead to increased surface area. The greater number of collisions at higher ball masses promotes smaller molecule formation and, consequently, a higher BET surface area.

4 Life cycle assessment of mechanosynthesis for PIM-1

4.1 Results of LCIA methods

The 18 midpoint indicators in ReCiPe have diverse units representing different categories, making comparisons between indicators complicated. However, normalization is employed to enhance the comparability of data and assessment results. Fig. S5† illustrated the overall analysis, whereas Fig. 3a highlights the most contrasting impact categories in the analysis. The wet chemical method has significantly larger environmental impacts compared to mechanosynthesis when synthesizing 1 g of PIM-1. Notably, global warming, ionizing radiation, and fossil fuel scarcity emerge as major impact categories, exhibiting significant differences in PIM-1 synthesis.

Global Warming Potential (GWP) is an indicator used to evaluate the impact of global warming. It represents the radiative energy emitted over time by 1 kg of greenhouse gas relative to the radiative energy emitted by 1 kg of CO_2, with the unit of kilograms of CO_2 equivalent (kg CO_2 eq.).[39] Ionizing radiation is characterized as a midpoint indicator relative to the radioactivity emitted by cobalt-60, a reference substance, to air, expressed in kilobecquerels of cobalt-60 equivalent (kBq Co-60 eq.).[39] Fossil fuel scarcity is assessed using fossil fuel potential, which represents the energy content of the fossil resource in the evaluated product system relative to the energy content in crude oil. The unit for this indicator is kilograms of oil equivalent (kg oil eq.).[39]

Fig. 3b demonstrates that the wet chemical synthesis method contributes 50% more to the global warming index compared to mechanosynthesis. In a study by Goh *et al.*, the global warming potential (GWP) was estimated to be approximately 2.5 kg CO_2 eq. for the synthesis of 1 g of PIM-1 *via* a wet chemical method.[28] In contrast, our findings indicate a GWP of around 12 kg CO_2 eq. A significant source of this discrepancy can be attributed to the data values associated with the raw materials. In our study, the data for raw materials, including TTSBI and TFTPN, was inferred based on elemental composition. Conversely, Goh *et al.* synthesized these raw materials from scratch, providing a more robust and reliable dataset. It is essential to note, however, that the primary objective of our study was to juxtapose the environmental ramifications of different synthesis methods, and not to provide a precise envrionmental impacts measure. Thus, potential inaccuracies arising from raw material data were considered secondary and were not the focal point of our analysis.

Similarly, Fig. 3c and d show that the wet chemical method has index values 1.5 times higher than mechanosynthesis for ionizing radiation and fossil fuel scarcity, respectively. This consistent trend across different impact categories suggests a common underlying cause, which will be further discussed in the next subsection.

4.1.1 Results interpretation. Global warming is primarily driven by human activities, such as the emission of greenhouse gases through fossil fuel combustion, deforestation, and industrial processes.[40] The wet chemical method exhibited a significantly higher global warming index compared to mechanosynthesis, as indicated by the midpoint analysis in Fig. 3a. This difference can be attributed to the substantial power consumption of the wet chemical method. In laboratory-scale experiments, the wet chemical method required approximately 8 h to complete, which was around 32 times longer than the reaction time of mechanosynthesis. Furthermore, the total power rating during the PIM-1 synthesis reaction was 0.1 kWh for the wet chemical method and 1.25 kWh for mechanosynthesis. Considering the extended duration of the reaction, the energy consumption was amplified for the wet chemical method. Consequently, utilizing the wet chemical method releases more energy into the environment, contributing to global warming.

On the other hand, the high impact value of ionizing radiation in the wet chemical method can be attributed to its high electricity consumption. In the UK, the 13 nuclear reactors that are currently operating contribute 20% of the country's electricity generation as of 2020.[41] Ionizing radiation is primarily generated through activities related to nuclear fuel mining, processing, waste disposal, as well as coal burning and phosphate rock extraction.[39] Even at low radiation concentrations, radiation exposure can have severe health consequences, particularly for pregnant women, including cancer, growth retardation, and impaired brain function.[42]

The wet chemical method significantly depletes non-renewable fossil resources faster compared to mechanosynthesis. Fossil fuels such as natural gas, petroleum, and coal are commonly used as sources for electrical power generation. These fuels are considered non-renewable resources, meaning they will become increasingly scarce over time unless alternative energy sources are adopted. The depletion of fossil fuel

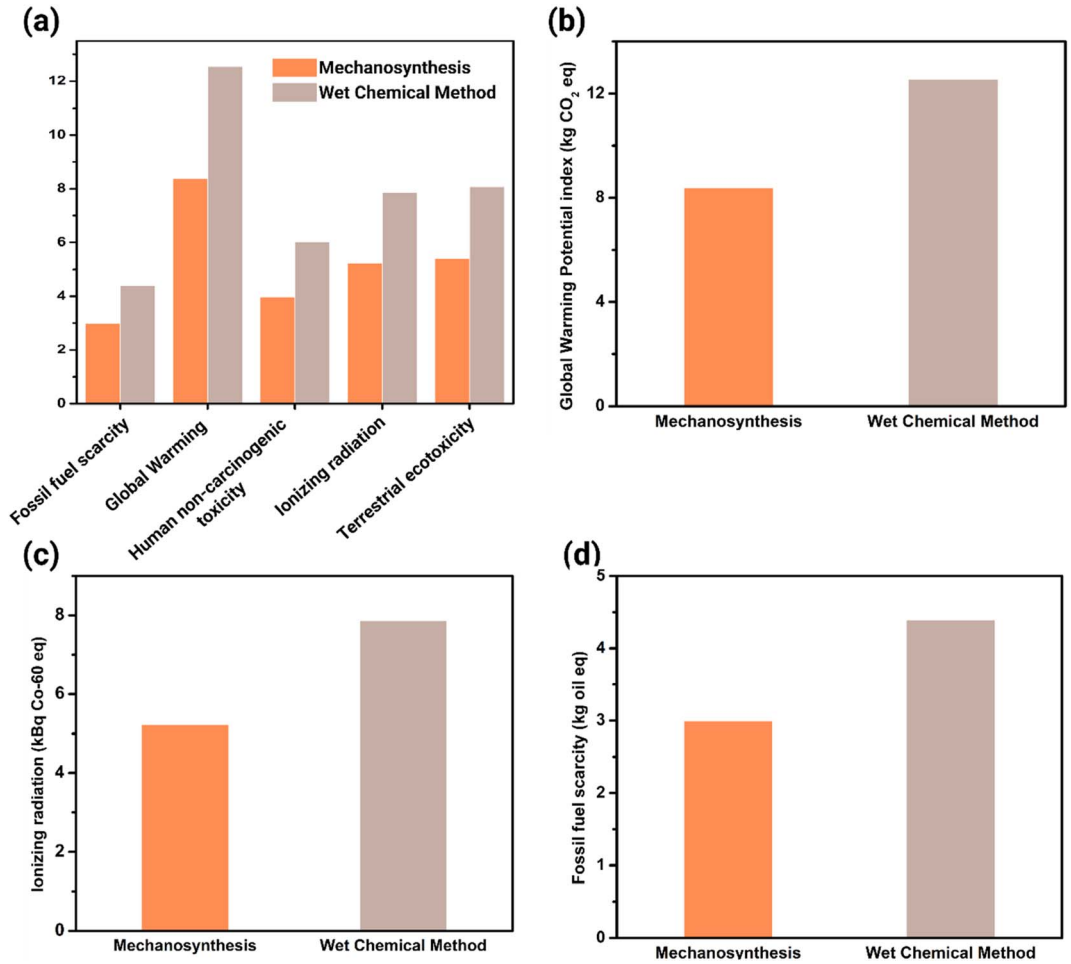

Fig. 3 Life cycle analysis for comparison of two methods (mechanosynthesis and wet chemical) for PIM-1 synthesis (a) normalised ReCiPe (2016) midpoint (H) analysis result, results on (b) global warming index, (c) ionising radiation index, and (d) fossil fuel scarcity index from ReCiPe analysis.

reserves can have severe consequences for humanity, including inflation and disparities in wealth distribution. Therefore, it is crucial to consider the scarcity of fossil fuels when comparing the two synthesis methods.

When comparing the wet chemical method and mechanosynthesis in LCA, it is important to consider factors beyond energy consumption, such as the involvement of solvents. According to the system boundary depicted in Fig. 1, the chemicals used in PIM-1 synthesis for both methods are sourced from mineral extraction to the final product manufacturing stages. The additional solvents utilized in the reaction stage of the wet chemical method, such as DMSO and toluene were likely to contribute to three or more environmental impacts. Moreover, the manufacturing and mineral extraction processes require additional electricity and labor, amplifying the overall impact. Furthermore, transportation stages following mineral extraction and manufacturing can contribute to greenhouse gas emissions, intensifying global warming. Taking these factors into consideration is crucial for a comprehensive assessment of the differences between the two synthesis methods.

In the context of PIM-1's mechanosynthesis, certain methodological adjustments could offer significant environmental benefits. From a toxicological perspective, the primary concerns—both non-carcinogenic and carcinogenic—are intimately linked to the organic solvents employed during purification. It's imperative, from both an academic and practical standpoint, to investigate strategies that reduce or optimize these solvent volumes. Concurrently, land use considerations, as delineated in standard LCA frameworks, must be scrutinized. The elevated land usage can be attributed to three pivotal factors: transportation logistics associated with raw materials, the protocols adopted for waste solvent disposal, and the infrastructure requisites of the reaction process. A holistic approach that encompasses rigorous logistical planning, transportation optimization, and methodological refinement in reactions can potentially address these environmental challenges.

4.1.2 Limitation. To enhance the quality of the life cycle assessment, it is important to acknowledge the limitations of this comparative analysis. Firstly, the primary chemical compounds involved in the synthesis, TTSBI and TFTPN, were not available in the Eco-Invent 3.7 database. This led to inaccuracies in calculating the environmental impacts of the reaction, which highly affected the outcomes of the assessment. Secondly, this LCA report was based on lab-scale experiments.

Therefore, the power ratings, energy inputs, and operating conditions of the equipment were not precise and optimized. For example, the power rating of the oven was assumed to be at its maximum capacity, which is unrealistic and could lead to an overestimation of environmental consequences. Additionally, the referenced literature only provides qualitative results for mechanosynthesis, lacking quantitative product yield data. These limitations should be taken into account when interpreting the results of the assessment.

5 Conclusion

Experimental results and life cycle analysis reported here compared and underscored the mechanism of mechanosynthesis and its environmental implication. By synthesizing PIM-1 under different operating parameters, including varying reaction times (20, 40, 60 min) and reactants to balls mass ratios (1 : 64, 1 : 128), the synthesis of PIM-1 samples has been confirmed through analyses. The synthesis of PIM-1 using mechanosynthesis, coupled with its positive environmental impact demonstrated through LCA, highlights the potential of this technique. The results of this assessment demonstrated that mechanosynthesis is generally more environmentally friendly, particularly in terms of energy usage and solvent involvement. Key environmental factors, such as fossil fuel scarcity, ionizing radiation, and global warming, were considered. However, further advancements are necessary to overcome existing limitations and optimize its implementation. The ongoing efforts in mechanosynthesis research hold promise for the development of a sustainable and efficient approach to chemical synthesis.

Conflicts of interest

There are no conflicts to declare.

Acknowledgements

C. Y. L. would like to thank the EPSRC for PhD studentship. R. H. would like to acknowledge the financial support from China Scholarship Council. Authors also thanked financial support from Royal Society of Chemistry (research fund R21-4839757049) and Royal Society International Exchange (IEC\NSFC\211021).

References

1 P. M. Budd, B. S. Ghanem, S. Makhseed, N. B. McKeown, K. J. Msayib and C. E. Tattershall, *Chem. Commun.*, 2004, 230–231, DOI: **10.1039/B311764B**.
2 N. B. McKeown and P. M. Budd, *Macromolecules*, 2010, **43**, 5163–5176.
3 B. Satilmis and T. Uyar, *Appl. Surf. Sci.*, 2018, **453**, 220–229.
4 S. H. Pang, M. L. Jue, J. Leisen, C. W. Jones and R. P. Lively, *ACS Macro Lett.*, 2015, **4**, 1415–1419.
5 N. B. McKeown, P. M. Budd, K. J. Msayib, B. S. Ghanem, H. J. Kingston, C. E. Tattershall, S. Makhseed, K. J. Reynolds and D. Fritsch, *Chem.–Eur. J.*, 2005, **11**, 2610–2620.
6 S. Rochat, K. Polak-Kraśna, M. Tian, T. J. Mays, C. R. Bowen and A. D. Burrows, *Int. J. Hydrogen Energy*, 2019, **44**, 332–337.
7 N. Du, G. P. Robertson, J. Song, I. Pinnau, S. Thomas and M. D. Guiver, *Macromolecules*, 2008, **41**, 9656–9662.
8 R. Ye, D. Henkensmeier, S. J. Yoon, Z. Huang, D. K. Kim, Z. Chang, S. Kim and R. Chen, *J. Electrochem. Energy Convers. Storage*, 2017, **15**, 10801.
9 J. Song, N. Du, Y. Dai, G. P. Robertson, M. D. Guiver, S. Thomas and I. Pinnau, *Macromolecules*, 2008, **41**, 7411–7417.
10 P. Zhang, X. Jiang, S. Wan and S. Dai, *J. Mater. Chem. A*, 2015, **3**, 6739–6741.
11 P. Baláž, M. Achimovičová, M. Baláž, P. Billik, Z. Cherkezova-Zheleva, J. M. Criado, F. Delogu, E. Dutková, E. Gaffet, F. J. Gotor, R. Kumar, I. Mitov, T. Rojac, M. Senna, A. Streletskii and K. Wieczorek-Ciurowa, *Chem. Soc. Rev.*, 2013, **42**, 7571–7637.
12 K. Horie, M. Barón, R. B. Fox, J. He, M. Hess, J. Kahovec, T. Kitayama, P. Kubisa, E. Maréchal, W. Mormann, R. F. T. Stepto, D. Tabak, J. Vohlídal, E. S. Wilks and W. J. Work, *Pure Appl. Chem.*, 2004, **76**, 889–906.
13 J. H. Yan, Z. Peng, S. Y. Lu, X. D. Li, M. J. Ni, K. F. Cen and H. F. Dai, *J. Hazard. Mater.*, 2007, **147**, 652–657.
14 Y. Nomura, K. Fujiwara, M. Takada, S. Nakai and M. Hosomi, *J. Mater. Cycles Waste Manage.*, 2008, **10**, 14–18.
15 Z. Chen, S. Lu, M. Tang, X. Lin, Q. Qiu, H. He and J. Yan, *Sci. Total Environ.*, 2019, **694**, 133813.
16 S. Mori, W. C. Xu, T. Ishidzuki, N. Ogasawara, J. Imai and K. Kobayashi, *Appl. Catal., A*, 1996, **137**, 255–268.
17 K. L. Chagoya, D. J. Nash, T. Jiang, D. Le, S. Alayoglu, K. B. Idrees, X. Zhang, O. K. Farha, J. K. Harper, T. S. Rahman and R. G. Blair, *ACS Sustainable Chem. Eng.*, 2021, **9**, 2447–2455.
18 C. V. Picasso, D. A. Safin, I. Dovgaliuk, F. Devred, D. Debecker, H.-W. Li, J. Proost and Y. Filinchuk, *Int. J. Hydrogen Energy*, 2016, **41**, 14377–14386.
19 M. Vakili, W. Qiu, G. Cagnetta, J. Huang and G. Yu, *Front. Environ. Sci. Eng.*, 2021, **15**, 128.
20 H. Li, M. Dai, S. Dai, X. Dong and F. Li, *Hum. Ecol. Risk Assess.*, 2018, **24**, 2133–2141.
21 D. Tian, X. Zhang, C. Lu, G. Yuan, W. Zhang and Z. Zhou, *Cellulose*, 2014, **21**, 473–484.
22 N. Fantozzi, J.-N. Volle, A. Porcheddu, D. Virieux, F. García and E. Colacino, *Chem. Soc. Rev.*, 2023, **52**, 6680–6714.
23 O. Galant, G. Cerfeda, A. S. McCalmont, S. L. James, A. Porcheddu, F. Delogu, D. E. Crawford, E. Colacino and S. Spatari, *ACS Sustainable Chem. Eng.*, 2022, **10**, 1430–1439.
24 O. Galant, A. Aborome, A. S. McCalmont, S. L. James, M. Patrascu and S. Spatari, *ACS Sustainable Chem. Eng.*, 2023, **11**, 12155–12165.
25 A. DeVierno Kreuder, T. House-Knight, J. Whitford, E. Ponnusamy, P. Miller, N. Jesse, R. Rodenborn, S. Sayag, M. Gebel, I. Aped, I. Sharfstein, E. Manaster, I. Ergaz, A. Harris and L. Nelowet Grice, *ACS Sustainable Chem. Eng.*, 2017, **5**, 2927–2935.

26 I. V. Muralikrishna and V. Manickam, in *Environmental Management*, ed. I. V. Muralikrishna and V. Manickam, Butterworth-Heinemann, 2017, pp. 57–75, DOI: 10.1016/B978-0-12-811989-1.00005-1.
27 A. Bjørn, M. Owsianiak, C. Molin and A. Laurent, in *Life Cycle Assessment: Theory and Practice*, ed. M. Z. Hauschild, R. K. Rosenbaum and S. I. Olsen, Springer International Publishing, Cham, 2018, pp. 9–16, DOI: 10.1007/978-3-319-56475-3_2.
28 W. H. D. Goh, H. S. Lau and W. F. Yong, *Sci. Total Environ.*, 2023, **892**, 164582.
29 I. I. Ponomarev, D. Y. Razorenov, I. V. Blagodatskikh, A. V. Muranov, L. E. Staranikova, A. Y. Alent'ev, R. Y. Nikiforov and Y. P. Yampol'skii, *Polym. Sci., Ser. B*, 2019, **61**, 605–612.
30 J. C. Bare and T. P. Gloria, *Environ. Sci. Technol.*, 2006, **40**, 1104–1113.
31 K. Polak-Kraśna, R. Dawson, L. T. Holyfield, C. R. Bowen, A. D. Burrows and T. J. Mays, *J. Mater. Sci.*, 2017, **52**, 3862–3875.
32 P. Zhang, X. Jiang, S. Wan and S. Dai, *J. Mater. Chem. A*, 2015, **3**, 6739–6741.
33 T. Friščić, *Chem. Soc. Rev.*, 2012, **41**, 3493–3510.
34 S. V. Gutiérrez-Hernández, F. Pardo, A. B. Foster, P. Gorgojo, P. M. Budd, G. Zarca and A. Urtiaga, *J. Membr. Sci.*, 2023, **675**, 121532.
35 R. S. Bhavsar, T. Mitra, D. J. Adams, A. I. Cooper and P. M. Budd, *J. Membr. Sci.*, 2018, **564**, 878–886.
36 H. J. Kim, D.-G. Kim, K. Lee, Y. Baek, Y. Yoo, Y. S. Kim, B. G. Kim and J.-C. Lee, *Sci. Rep.*, 2016, **6**, 36078.
37 J. Jeromenok and J. Weber, *Langmuir*, 2013, **29**, 12982–12989.
38 N. B. McKeown and P. M. Budd, *Chem. Soc. Rev.*, 2006, **35**, 675–683.
39 M. A. J. Huijbregts, Z. J. N. Steinmann, P. M. F. Elshout, G. Stam, F. Verones, M. Vieira, M. Zijp, A. Hollander and R. v. Zelm, *Int. J. Life Cycle Assess.*, 2017, **22**, 138–147.
40 S. R. Weart, *The Discovery of Global Warming*, Harvard University Press, 2008.
41 S. Jack, New nuclear plant at Sizewell set for green light, https://www.bbc.co.uk/news/business-54754016, accessed 6 August 2021.
42 N. F. Abu Bakar, S. Amira Othman, N. F. Amirah Nor Azman and N. Saqinah Jasrin, *IOP Conf. Ser. Earth Environ. Sci.*, 2019, **268**, 012005.